Remote Sensing in Ecology and Conservation
Open Access
ZSL LET'S WORK FOR WILDLIFE

ORIGINAL RESEARCH

Simultaneous monitoring of vegetation dynamics and wildlife activity with camera traps to assess habitat change

Catherine Sun[1], Christopher Beirne[1], Joanna M. Burgar[1,2], Thomas Howey[1], Jason T. Fisher[2] & A. Cole Burton[1]

[1]Department of Forest Resources Management, University of British Columbia, 2424 Main Mall, Vancouver V6T 1Z4, Canada
[2]School of Environmental Studies, University of Victoria, Victoria, V8W 2Y2, Canada

Keywords
Animal ecology, disturbance, phenology, productivity, remote camera, satellite

Correspondence
Catherine Sun, Department of Forest Resources Management, University of British Columbia, 2424 Main Mall, Vancouver, Canada V6T 1Z4. E-mail: catherine.c.sun@gmail.com

Editor: Marcus Rowcliffe
Associate Editor: Tim Hofmeester

Received: 20 January 2021; Revised: 7 May 2021; Accepted: 13 May 2021

doi: 10.1002/rse2.222

Abstract

Vegetation phenology and productivity drive resource use by wildlife. Vegetation dynamics also reveal patterns of habitat disturbance and recovery. Monitoring these fine-scale vegetation patterns over large spatiotemporal extents can be difficult, but camera traps (CTs) commonly used to survey wildlife populations also collect data on local habitat conditions. We used CTs (n = 73) from 2016 to 2019 to assess impacts of habitat change in a boreal landscape of northern Canada, where seismic lines for petroleum exploration disturbed wildlife habitat and prompted vegetation restoration efforts. First, we quantified vegetation dynamics from CTs, comparing them to satellite-based estimates that are typically used to monitor vegetation at broad spatial scales. We then used understory phenology and productivity estimated from CT time-lapse images to assess vegetation recovery on seismic lines. Finally, we related vegetation dynamics with the habitat use of three wildlife species: sandhill cranes *Grus canadensis*, woodland caribou *Rangifer tarandus*, and white-tailed deer *Odocoileus virginianus*. CTs provided unique insight into vegetation dynamics that were different from signals measured by satellites, with temporally inconsistent and even some negative correlations between CT and satellite metrics. We found some indication of vegetation recovery on seismic lines that had received restoration treatment, with understory patterns more similar to undisturbed habitat than to seismic lines that did not receive restoration treatment. CTs also provided inferences about wildlife activity related to vegetation resources, which approaches using satellite data failed to detect. Wildlife habitat use tracked vegetation phenology, but did not always increase with vegetation productivity at weekly, 16-day, or annual intervals. Instead, associations with vegetation productivity depended on species, temporal scale, and productivity metrics. Given the widespread and growing use of CTs to monitor terrestrial wildlife, we recommend their use to simultaneously monitor habitat conditions to better understand the mechanisms that govern wildlife habitat use in changing environments.

Introduction

Wildlife respond to temporal and spatial patterns in habitat conditions to survive and complete their life cycles. For example, many northern species molt with shortening day-length to maintain camouflage from predators during winter conditions (Mills et al., 2018; Zimova et al., 2018). Herbivores track seasonal forage, such as the moving front of emerging spring vegetation (i.e., "surfing the green wave"; Merkle et al., 2016) or periodic flushes in flowering and fruiting (Armstrong et al., 2016; Sakai & Kitajima, 2019). In turn, predators track herbivores. Vegetation phenology (timing) and productivity (quantity) can thus reflect forage quantity and quality that influence how wildlife use habitat (Gentry & Emmons, 1987; Iversen et al., 2014). When natural and anthropogenic

changes modify the phenology and productivity of resources such as forage (Visser & Both 2005), wildlife must move, adapt, or risk reduced fitness and survival (Zimova et al., 2016). Monitoring vegetation dynamics is key to understanding how wildlife use resources and for conserving biodiversity under habitat change.

Camera trapping has typically focused on sampling wildlife (Burton et al., 2015), and is increasingly used to also sample local, ground-level habitat conditions (Bater et al., 2011; Ide & Oguma, 2010; Sirén et al., 2018). Accordingly, the scalability and cost-efficiency (Steenweg et al., 2017) of camera traps (CTs) have created new opportunities for linking wildlife to resource conditions (e.g., Hofmeester et al., 2019). Networks or arrays of CTs can potentially monitor vegetation more frequently with automated data collection compared with repeated manual measurements of, for example of stem counts (Filicetti et al., 2019) or vegetation green-up (Denny et al., 2014). To achieve a similar temporal resolution, manual sampling with limited resources would be spatially restricted to smaller extents or fewer sampling locations. Conversely, above and near-ground sensing with satellites (Zhang et al., 2003), unmanned aerial vehicles (Ancin-Murguzur et al., 2020; Tóth, 2018), and phenocams (Seyednasrollah et al., 2019) can increase spatial coverage but often with coarser spatial or temporal resolution (Zeng et al., 2020). Above and near-ground remote sensing of understory signals are also subject to physical obstruction and bias by canopy vegetation (Lopatin et al., 2019; Tuanmu et al., 2010), which have their distinct dynamics (Richardson & O'Keefe, 2009). Thus, ground-level CTs are a promising method for balancing temporally continuous and spatially extensive monitoring for understory vegetation.

Monitoring vegetation and biodiversity is important given rapid habitat change characteristic of the Anthropocene (Lewis & Maslin, 2015). Habitat loss and degradation can shift vegetation composition, phenology, and productivity (Sankey et al., 2013), portending declines in ecosystem function and mismatched species interactions (Doyle et al., 2020; Morellato et al., 2016; Torre Cerro & Holloway, 2020). Subsequent habitat recovery and restoration may be characterized by changes in vegetation dynamics due to early seral vegetation growth, plant succession (Connell & Slatyer, 1977; Finnegan et al., 2018), and wildlife activity returning to reference conditions (Gann et al., 2019; Miller & Hobbs, 2007). Thus, linking vegetation dynamics and wildlife activity is essential for assessing habitat change and restoration effectiveness (Alberton et al., 2017; Buisson et al., 2017; Walker & Soulard, 2019).

Canada's boreal forests provide critical ecosystem functions and services including carbon sequestration and wildlife habitat, yet they are increasingly transformed by industrial disturbance (Bradshaw et al., 2009; Schindler & Lee, 2010), including mining and logging (Robinne et al. 2016). In particular, linear features cut for petroleum exploration (i.e., seismic lines) have disturbed >1.5 million km^2 of forest and wetlands in northern Alberta and occur at a mean density of 1.5 km/km^2 (Dabros et al., 2018; Lee & Boutin, 2006), contributing to a novel landscape with widespread anthropogenic manipulation and disturbances (Pickell et al., 2015). Extensive coverage of seismic lines and their slow habitat recovery have had varying effects on wildlife species (Fisher & Burton, 2018; Mahon et al., 2019; Wittische et al., 2021). Notably, seismic lines have caused declines in woodland caribou *Rangifer tarandus* (Hebblewhite, 2017; Hervieux et al., 2013), which are federally listed as threatened in Canada (Canada & Environment Canada, 2015). Caribou face increased predation from wolves *Canis lupus* that travel farther and faster on the treeless, compacted terrain of seismic lines (Dickie et al., 2017, 2019; McKenzie et al., 2012), and experience apparent competition with other prey species including moose *Alces alces* and range-expanding white-tailed deer *Odocoileus virginianus* (Dawe et al., 2014; Fisher et al., 2020; Latham et al., 2011). Returning vegetation on seismic lines to undisturbed conditions is therefore critical to restoring wildlife interactions (Filicetti et al., 2019). However, restoration effectiveness has not been well studied, with scant evidence of short-term success based on coarse descriptions of habitat conditions [e.g., anthropogenic vs. natural, restoration treatment vs. no treatment (Fisher & Burton, 2018; Serrouya et al., 2020; Tattersall et al., 2020a)]. Assessing early habitat responses following restoration efforts has also been hampered by slow tree growth (Finnegan et al., 2019; Lupardus et al., 2019). Dynamics of early seral vegetation, instead, may be more discriminating of initial vegetation patterns that impact wildlife and the trajectory of habitat recovery.

Here, we demonstrate how CTs can simultaneously measure early seral and understory vegetation dynamics (phenology and productivity) and wildlife activity to assess impacts of habitat change. We capitalized on a multiyear CT study of wildlife on seismic lines in boreal forests of northern Canada. First, we established the feasibility and value of quantifying vegetation dynamics from CTs, using an automated extraction method and compared results to those from common satellite datasets. We anticipated weak similarities between CT and satellite-based metrics due to the different components of vegetation structure that they capture (Table 1). Second, we examined vegetation conditions on seismic lines following restoration treatment by comparing their understory vegetation dynamics to undisturbed reference conditions

Table 1. Summary of the three objectives related to vegetation dynamics and linkages to habitat disturbance and wildlife activity, with associated hypotheses and predictions addressed with CT images from n = 73 CT sites in the study area in northern Alberta, Canada, from January 2016 to November 2019.

Objective	Hypotheses	Associated predictions	References
Quantifying and comparing vegetation dynamics	CTs and satellites captured dynamics of different components of vegetation structure – understory/early seral and canopy, respectively.	CT and satellite metrics would be positively but weakly correlated	Richardson and O'Keefe (2009), Lopatin et al. (2019) and Tuanmu et al. (2010)
Impacts on vegetation dynamics: disturbance and restoration	Anthropogenic disturbance and restoration altered vegetation dynamics on seismic lines, with areas off seismic lines retaining undisturbed vegetation conditions	Length of growing season and DHI values would increase from lowest to highest, from unrestored Human Use/Control to Active to Passive sites on seismic lines.	Steinaker et al. (2016) and Emmett et al. (2019)
		Offline sites would have the longest growing seasons, largest DHI values, and most consistent green-up and senescence dates across years	
Linking wildlife habitat use to vegetation dynamics	Timing and use of habitat use by wildlife were related to understory and early seral vegetation to due forage availability	Phenology: Migratory crane detections would be concordant with the vegetation growing season, while resident deer and caribou detections would extend past the growing season.	Rettie and Messier (2001) and Hobson et al. (2006)
		Productivity: Species' detections would temporally increase with greenness and be more numerous at sites with greater greenness	Mueller et al. (2008) and Razenkova et al. (2020)
		Effect sizes would be greater for deer than for caribou	Dawe et al. (2014) and Fisher et al. (2020)
	Due to forage needs, terrestrial wildlife depended on understory and early seral vegetation more than canopy vegetation	Species detections would be better explained by greenness from CTs than satellites	Pauley et al. (1993) and Lone et al. (2014)

(Table 1). We predicted that sites that received restoration and had regenerating vegetation would have longer growing seasons and greater vegetation productivity. Finally, we tested links between understory vegetation dynamics and wildlife habitat use, focusing on three species that rely on understory vegetation and differ in ecological and conservation characteristics: migratory sandhill crane *Grus canadensis*, threatened woodland caribou, and range-expanding white-tailed deer (Table 1). We predicted: (1) the annual timing of crane detections would be concordant with the vegetation growing season given their seasonal presence and dependence on boreal breeding habitat (Hobson et al., 2006), while detections of resident deer and caribou would occur across seasons due to their year-round activities including foraging, calving, rutting, and seasonal movements (Rettie & Messier, 2001); (2) habitat use by all species would increase with vegetation productivity throughout the year, particularly for deer given their dependence on early seral forage; and (3) annual habitat use over the landscape for all species would be greater in areas with more vegetation productivity.

Materials and Methods

Study area

The 570 km^2 study area in northern Alberta (Fig. 1) lay within the Athabasca Oil Sands Region and the range of the East Side Athabasca River woodland caribou population. Inactive seismic lines from petroleum exploration were the most significant anthropogenic disturbance, with an average density of 1.1 km/km^2 (Lee & Boutin, 2006; Tattersall et al., 2020a). Habitat restoration had occurred from 2011 to 2015 on approximately 264 ha of seismic lines originating as far back as the 1970s (Nexen & Silvacom, 2015). Restoration treatments involved either an "active" approach by actively planting 400–1,200 stems/ha of black spruce *Picea mariana* seedlings in addition to mechanical mounding of soil and application of coarse woody materials, or a "passive" approach by protecting natural regeneration of plants $\geq$1.5 m in height and >50% crown cover by application of coarse woody materials at the beginning of seismic lines to block access by people. Boreal habitat included lowland terrain (58%)

with fens, bogs, and mesic upland forests (31%) with primarily tamarack *Larix laricina*, aspen *Populus tremuloides* and balsam poplar *Populus balsamifera*, white and black spruce *Picea glauca, P. mariana*, and jack pine *Pinus banksiana* tree species (Burton et al. 2017). Understory vegetation included Labrador tea *Ledum groenlandicum*, wild rose *Rosa acicularis*, and bog rosemary *Adromeda polifolia*. Elevation ranged from 333 to 562 m, with a mean of 502 ± 36 m (standard deviation, SD); slope ranged from 0 to 0.8°, with a mean of 0.04 ± 0.0° (1SD); aspect ranged from 0 to 360° (1 SD of 105°).

We deployed n = 73 Reconyx PC900 HyperFire cameras (Holmen, WI, USA) between November 2015 and November 2019 to assess the effects of seismic line restoration treatment on predator use and mammal community structure (Tattersall et al. 2020a). Each site consisted of an un-lured CT set approximately 1 m high on a tree facing across a seismic line (but also facing north as much as possible to avoid false triggers). Sixty CTs were set across four sampling strata in a stratified random design (Table 2): "Active" sites (n = 22) that had received planting-based restoration treatment, "Passive" sites (n = 12) with only protection-based treatment, "Human Use" sites (n = 14) left untreated for access by human resource-users (e.g. trappers, energy workers), and "Control" sites (n = 12) designated for restoration but left as untreated controls. A fifth stratum of randomly selected "Offline" sites (n = 13) was added in November 2017 on game trails in undisturbed areas ≥100 m from seismic lines as a reference assumed to reflect end-goal vegetation conditions after complete, successful habitat restoration. Sites represented upland forest, lowland forest, and non-forested habitats roughly in proportion to their presence on the landscape at the 250 m resolution, with a mean elevation of 518 ± 14 m (mean ± 1 SD) (range: 484–576 m), mean slope of 0.01 ± 0.01° (range: 0–0.09°), and aspect that ranged from 11 to 360° with a SD of 97° (Table 2). CTs operated continuously, taking one image per motion trigger with no delay between triggers and daily time-lapse images at 12:00 PM to record functionality and daily local environmental conditions. We visited CTs to collect data each spring and fall.

We used CT time-lapse and wildlife images taken during 2016–2019, excluding 2015 to focus on annual cycles. We identified wildlife species in images using Camelot software (Hendry & Mann, 2018). Detections of a species per site were aggregated into a single independent detection event if they occurred ≤30 min, and considered separate events when >30 min apart (Rovero & Zimmermann, 2016).

Quantifying and comparing vegetation dynamics

Our first objective was to evaluate the utility of CTs for characterizing the dynamics of understory vegetation (including early seral vegetation, i.e., below the tree canopy) (Table 1). We used the "phenopix" package (Filippa et al., 2016) in program R (R Core Team, 2019) and focused on the foreground in time-lapse images, where terrestrial wildlife interact with understory vegetation, by delineating the region with a quadrilateral (Fig. S1). We redrew quadrilaterals for each period between field visits because CT handling during visits may have changed fields of view. We calculated a relative greenness index per time-lapse image averaged over the red, green, and blue values extracted across pixels within the quadrilateral, which we assumed to be representative of the local vegetation and greenness conditions even beyond the immediate view of the CT. We filtered greenness indices to remove noise and outliers using "phenopix" default parameter values, and fit a smoothing spline with the "splinefit" function to all years with ≥220 time-lapse images (i.e., >60% of the annual growth cycle) for each CT site (Fig. S2).

We calculated annual vegetation phenology and productivity metrics from splines (Table 3). For phenology, we defined onset dates of vegetation green-up and senescence as the earliest and latest dates that greenness reached 15% and 90% of the maximum value, respectively (Bolton et al., 2020). Growing season length was calculated as the number of days between green-up and senescence. For productivity, we used greenness index values as site-specific proxies (Moore et al. 2016; Toomey et al. 2015). While Westgaard-Nielsen et al. (2017) found that the relationship between greenness and productivity is site- and camera model- specific, our standardized camera set up (e.g., height, angle, make, and model) allowed for comparison of greenness values across sites. To characterize annual vegetation productivity, we calculated at each site a Dynamic Habitat Index (DHI; Coops et al., 2008; Radeloff et al., 2019), composed of three components of site-specific greenness: maximum greenness (rather than minimum values in the original formulation due to lack of variation in minimum values), cumulative greenness, and seasonality of greenness; these

Figure 1. Location of the study area in northern Alberta, Canada, with an inset showing the location of n = 73 camera trap sites across 5 sampling strata that collected wildlife detections and daily time-lapse images between November 2015 and November 2019. Major habitat distinctions and seismic lines are also shown.

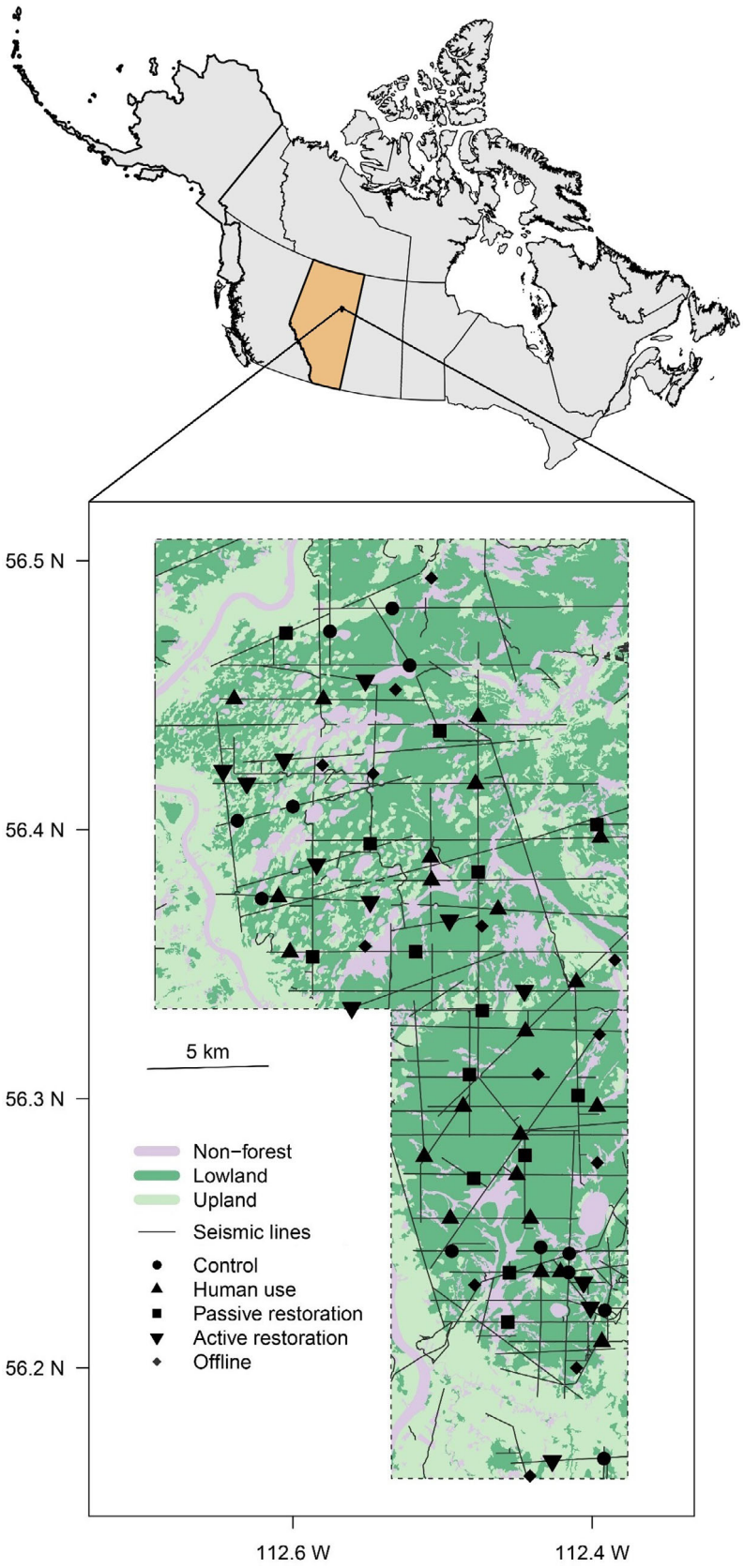

Table 2. Characterization of sampling strata, habitat type, and topography (mean ±1 SD) of n = 73 CT sites in the study area in northern Alberta, Canada, from January 2016 to November 2019.

Stratum	Sites (n)	Lowland	Upland	Non-forest	Elevation (m)	Slope (°)	Aspect (°)
Control	12	10	1	1	516 ± 1.0	0.02 ± 0	168 ± 9
Human use	14	11	0	3	517 ± 0.8	0 ± 0	173 ± 7
Passive	12	8	4	0	513 ± 0.7	0.01 ± 0	171 ± 10
Active	22	20	0	2	517 ± 0.5	0.01 ± 0	201 ± 4
Offline	13	10	1	2	517 ± 0.8	0.01 ± 0	127 ± 7

were calculated as the peak value, area under the curve, and coefficient of variation across daily values, respectively, for each annual spline.

For comparison, we calculated the same vegetation phenology and productivity metrics using satellite data at two spatiotemporal scales (Table 3). We obtained normalized difference and enhanced vegetation indices (NDVI, EVI) per site at 250 m resolution and 16-day frequency from the MOD13Q1 v6 product (Didan, 2015), using the "MODISTools" package (Tuck et al. 2014) in program R. NDVI quantifies vegetation based on chlorophyll pigment content and internal leaf structure from red and near-infrared spectral bands (Zeng et al., 2020); EVI better accounts for atmospheric and canopy background noise with an additional blue spectral band (Hobi et al., 2017). We fit splines to NDVI and EVI values to derive the same metrics described above. We included another set of metrics derived from finer-scale EVI2 data at 30 m resolution and 1–4 day frequency from harmonized Landsat 8 and Sentinel 2 (HLS2; Bolton et al., 2020) (Table 3). EVI2 is similar to EVI but does not use the blue band (Jiang et al., 2008). We calculated Pearson correlation coefficients between CT and satellite metrics annually across all sites and across years. Hereafter, we refer to "CT metrics" and "satellite metrics" as reflecting understory vegetation and canopy patterns, respectively.

Table 3. Annual vegetation phenology and productivity metrics extracted from camera trap (CT) time-lapse images and satellite-based products for n = 73 CT sites in the study area in northern Alberta, Canada, from January 2016 to November 2019.

	Camera Trap (CT)	NDVI (250 m)	EVI (250 m)	EVI2 (30 m)
Source	Ground	Satellite (MODIS)	Satellite (MODIS)	Satellite (Landsat + Sentinel 2)
Timeframe	2016–2019	2016–2019	2016–2019	2016–2018
Frequency	Daily	16-day	16-day	Annual (1–4 days)
Phenology				
Date of green-up	✓	✓	✓	
Date of senescence	✓	✓	✓	
Length of growing season	✓	✓	✓	
Productivity				
Maximum greenness (DHI)	✓	✓	✓	✓
Cumulative greenness(DHI)	✓	✓	✓	✓
Seasonality (DHI)	✓	✓	✓	
Amplitude				✓

Dates refer to the onset of phenology events, with the length of growing season as the difference in days. Maximum greenness is the peak value during each annual cycle; total greenness is the area under each annual greenness curve; seasonality is the coefficient of variation across daily values; amplitude is the difference in maximum and minimum values in each annual cycle. Maximum greenness, cumulative greenness, and seasonality of annual curves are adapted components of the Dynamic Habitat Index (DHI; Coops et al., 2008; Radeloff et al., 2019), which originally used minimum rather than maximum greenness.

Impacts on vegetation dynamics: disturbance and restoration

Our second objective was to assess understory vegetation conditions on seismic lines with CT metrics (Table 1). We predicted that CT metrics would detect differences in understory vegetation according to sampling strata, with sites on seismic lines having vegetation patterns distinct from the undisturbed, Offline sites, but with Active and Passive sites more similar to Offline sites than either Control or Human Use sites. We modeled annual green-up and senescence dates and growing season length as functions of the sampling strata, using generalized linear mixed models with CT site and year as random intercepts to account for non-independence (Table S1). We also modeled the consistency in green-up and senescence dates across years (i.e., range between earliest and latest dates across years when converted to day-of-year) as functions

of sampling strata (Table S1). We then compared DHI components across sampling strata using two-sample t tests with Bonferroni adjustments for multiple tests (Table S1).

Linking wildlife habitat use to vegetation dynamics

Finally, we linked crane, caribou, and deer detections to vegetation dynamics, using the number of independent CT detection events per species as a measure of relative habitat use (Table 1). We assumed similar and high detection probability across sampling strata of the focal species given their relatively large body sizes and the use of independent CT detections events rather than the number of raw CT detections (Fig. S3). To investigate vegetation phenology, we evaluated the concordance between annual periods of habitat use by each species with annual timings of the vegetation growing season estimated by CTs. We modeled the lack of concordance (in days) between each species' first detection and green-up, and between species' last detection and senescence (Table S1). We limited analyses to sites with $\geq$5 detections for cranes and deer, and $\geq$2 detections for caribou to focus on patterns of repeat habitat use and to minimize one-off detections from transient movement. Species-specific thresholds were determined based on plotting the lack of concordance between phenology and wildlife detection dates from sites with successively more detections of the species (Fig. S4).

We then investigated temporal and spatial patterns of habitat use related to vegetation productivity, using generalized linear mixed models with negative binomial response distributions. We modeled temporal patterns with weekly and 16-day counts of detections as functions of greenness measured from CTs (Table S1) and also EVI in 16-day count models. NDVI was not considered due to high correlation with EVI (NDVI: $r^2 > 0.50$), and EVI2 was not available for 2019. We included an offset of the (log) number of days that CTs operated to account for variable sampling effort. Model sets included all possible additive linear combinations of greenness predictors. We selected models with the lowest AICc (Tables S2–S5).

Lastly, we assessed spatial patterns of habitat use related to vegetation productivity. Per species, we modeled site-specific annual counts of detections (i.e., Jan–Nov/Dec) as functions of DHI components and growing season length estimated from CTs, NDVI, and EVI (Table S1). We used a multi-stage approach rather than a stepwise approach (Whittingham et al. 2006) to reduce the number of possible models and facilitate assessment of the relative impacts of the vegetation predictors. Specifically, we first constructed initial model sets for CTs, NDVI, and EVI each, consisting of all additive linear combinations of their respective predictors (Tables S6–S9). Top predictors per model set were determined as those with 95% CI that did not overlap 0 and $\leq$2 AICc of the top ranking (lowest AICc) model. We similarly evaluated and identified top covariates describing lowland habitat, sampling strata, and seismic line features to control for habitat and anthropogenic disturbance (Tables S10–S11, Supplementary Text). A final model per species included all orthogonal ($r^2 < 0.5$), best-supported productivity predictors and habitat and anthropogenic covariates.

For the count models, we identified the most supported variance formulation (quadratic or linear) of the negative binomial distribution using AICc model selection. We considered zero inflation and hurdle models to further address potential overdispersion (Tables S2, S4, S6, and Supplementary Text). For final models, we calculated the Ω^2 statistic, a measure of goodness of fit that compares the residual variances to that of the null model (Xu, 2003). Models were evaluated with "glmmTMB" (Brooks et al. 2017), "MuMIn" (Barton, 2020), and "AICmodavg" (Mazerolle, 2019) packages in program R.

Results

Quantifying and comparing vegetation dynamics

Using CTs, date of green-up was 24 April $\pm$1.4 days (mean $\pm$ 1 standard error) (range: 8 March–4 June) across all sites and years. Date of senescence was 13 August $\pm$1.6 days (range: 13 June–13 September). Notably, CT and satellite metrics of vegetation dynamics differed, with variable but generally low and even negative correlations. Annual correlations across sites had a mode value of $r = -0.23$ (range: -0.68 to 0.72; inner quartile range: -0.14 to 0.15). Across years, only 13 of 44 correlations were significant ($P < 0.05$; Fig. 2). Of the CT metrics, seasonality of greenness was significantly correlated every year with satellite metrics, but had the largest range and therefore inconsistencies in correlation (2018: $r = -0.68$ with amplitude of EVI2, $P < 0.001$; 2016: $r = 0.72$ with cumulative EVI2, $P < 0.001$). The most distinctive CT metric was maximum greenness, correlating the least frequently, and on average the most weakly, with satellite metrics across years (Fig. 2).

Impacts on vegetation dynamics: disturbance and restoration

Vegetation dynamics across sampling strata were similar according to CT metrics, but with some differences suggestive of understory recovery (Fig. 3). As predicted,

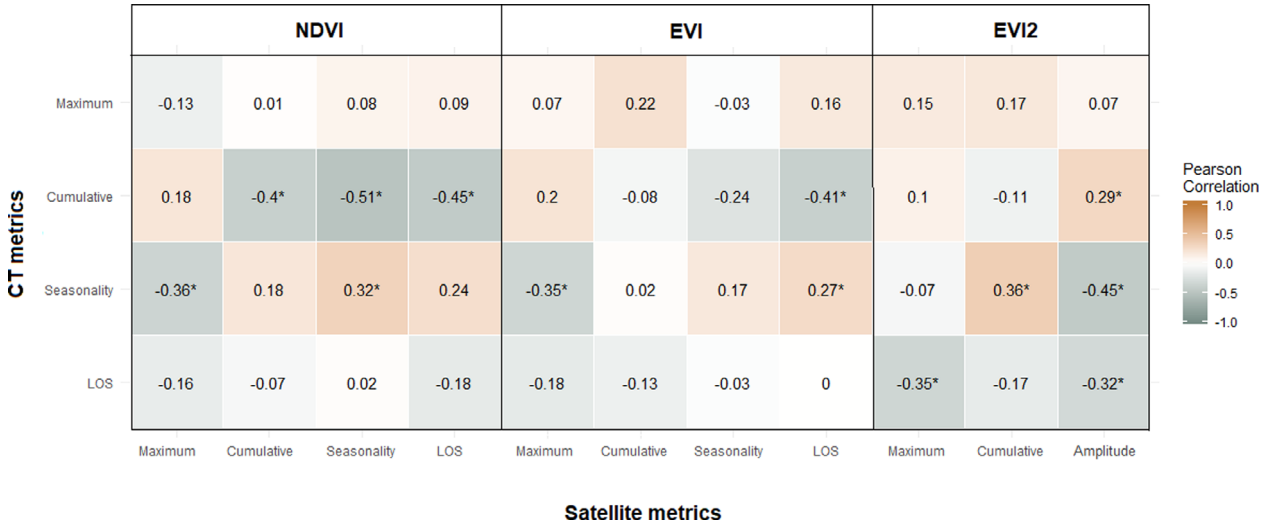

Figure 2. Pearson correlations between CT (camera trap) and satellite-based phenology and productivity metrics, across n = 73 CT sites and years in the study area in northern Alberta, Canada, from January 2016 to November 2019. Metrics included annual values of maximum, cumulative, and seasonality of greenness, length of annual growing season (LOS), and annual amplitude (Amplitude) of the greenness cycle. Comparisons with EVI and NDVI are for the entire 2016–2019 study period; comparisons with EVI2 are for 2016–2018. Asterisks indicate statistical significance at the $\alpha = 0.05$ level.

Offline sites had the longest growing season, due to the earliest mean green-up date (13 April ±4 days) and latest mean senescence date (19 August ±2 days). Passive sites had similar dates, and thus growing season length, to the Offline reference conditions. Active sites and unrestored Human Use and Control sites had shorter growing seasons ($P < 0.01$) (Fig. 3A). Specifically, Human Use and Control sites had significantly later green-up by 16 ± 5 ($P < 0.01$) and 20 ± 5 days ($P < 0.01$), respectively, while Active and Control sites had significantly earlier senescence by 8 ± 4 ($P = 0.04$) and 10 ± 5 ($P = 0.03$) days, respectively. Active and Passive sites had inconsistent senescence dates across years, ranging an additional 20 ± 6 ($P < 0.01$) and 13 ± 5 ($P < 0.01$) days, respectively, compared with Offline sites (5 ± 4 days, $P = 0.17$). Sampling strata were indistinguishable according to two DHI components: cumulative greenness and seasonality of greenness (Fig. 3B). However, maximum greenness was lower at Offline sites (542 ± 34) than at Active (753 ± 43, $P < 0.001$) and Control sites (787 ± 60, $P < 0.001$).

Linking wildlife habitat use to vegetation dynamics

Crane, caribou, and deer were detected in all sampling strata and in all habitat types (Table S12). Cranes were detected a total n = 1,476 times from 2016 to 2019 (n = 201, 299, 358, and 618 in successive years); deer were detected n = 1,786 times (n = 246, 323, 437, and 780 in successive years); caribou were detected n = 469 times (n = 52, 88, 143, and 186 in successive years). Annual timings of crane, caribou, and deer detections across sites and years were concordant with vegetation phenology measured by CTs. Cranes were detected within the growing season, shortly after green-up (5 ± 9 days after, $P = 0.54$) until 14 ± 7 days ($P = 0.05$) before senescence (Fig. 4, Fig. S5). By contrast, caribou and deer were detected throughout each year (Fig. 4, Fig. S5), although post-hoc chi-squared tests indicated their detections occurred more during the average growing season than expected based on season length and accounting for camera operation ($X^2_{\text{deer}} = 221.56$, $X^2_{\text{caribou}} = 199.36$; d.f. = 1, $P < 0.01$). Caribou detections past the growing season were most pronounced at Human Use sites (n = 84, 58 ± 26 days after senescence, $P = 0.03$; Fig. S6).

Habitat use by the three wildlife species did not always increase temporally or spatially with vegetation productivity, contrary to predictions. Also, concordance was not always greater with CT metrics than with satellite metrics. Instead, habitat use patterns depended on species, temporal scale, and choice of metric. For all species, weekly counts of detections increased with greenness measured by CTs ($\beta_{\text{crane}} = 0.76 \pm 0.04$, $P < 0.01$; $\beta_{\text{caribou}} = 0.64 \pm 0.06$, $P < 0.01$; $\beta_{\text{deer}} = 0.37 \pm 0.03$, $P < 0.01$) (Fig. 5). However, 16-day counts did not increase with greenness measured by CTs and increased instead with

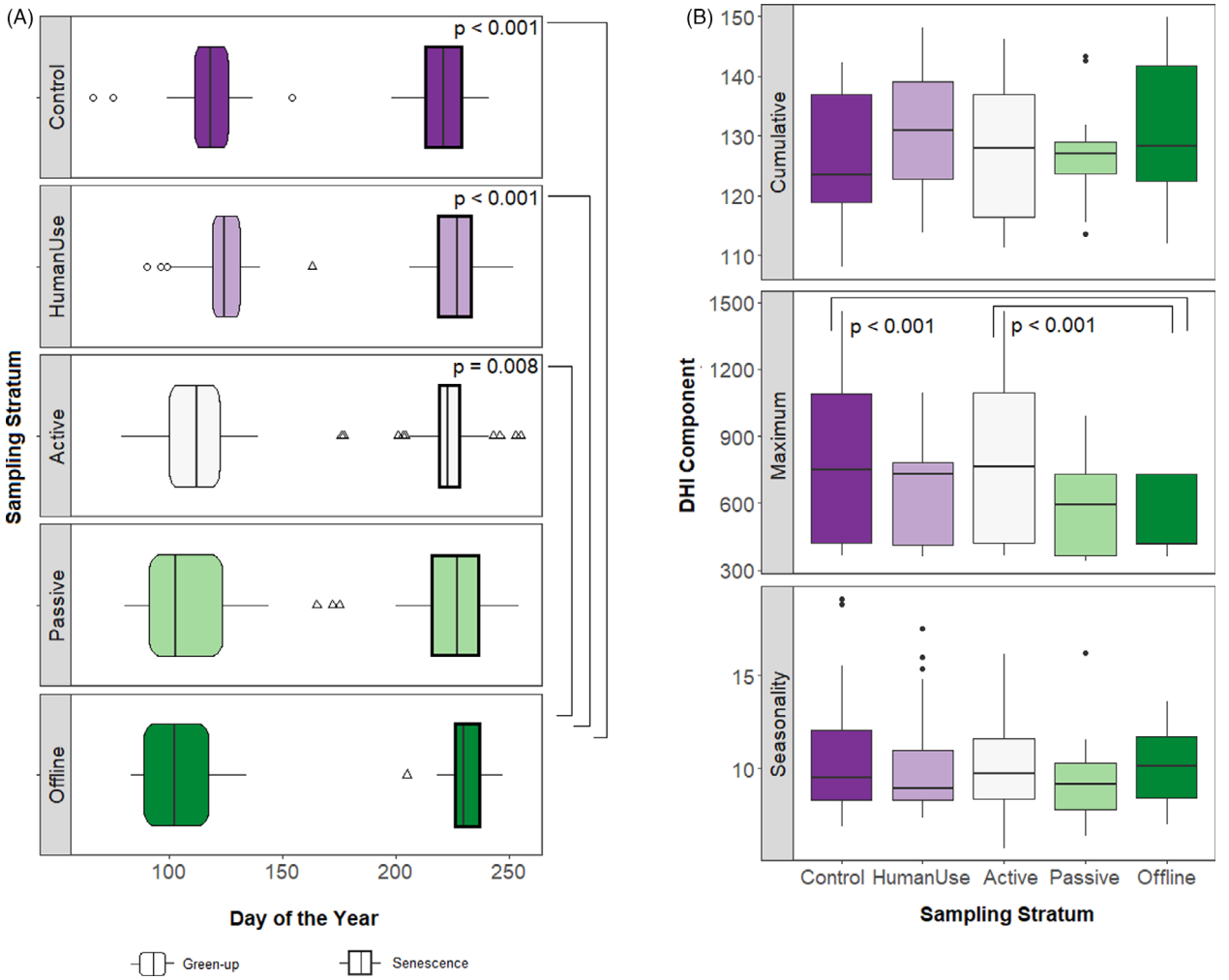

Figure 3. Comparisons across sampling strata of (A) green-up and senescence dates, with outliers for each respectively represented by circles and triangles, and (B) DHI components extracted from n = 73 camera traps at sites in the study area in northern Alberta, Canada from January 2016 to November 2019. DHI components included cumulative greenness (calculated as the area under annual curves) maximum greenness (peak value in annual curves), seasonality of greenness within each year (coefficient of variation across daily values). Statistically significant differences across sampling strata are indicated with *P*-values.

EVI ($\beta_{crane} = 2.26 \pm 0.15$, $P < 0.01$; $\beta_{caribou} = 0.84 \pm 0.08$, $P < 0.01$; $\beta_{deer} = 0.63 \pm 0.09$, $P < 0.01$) (Fig. 5). Also contrary to predictions, greenness had a greater effect size on caribou counts than on deer counts. Final models for crane, caribou, and deer had low explanatory power, with Ω^2 statistics of 0.16, 0.09, and 0.23 at the weekly scale, respectively, and 0.04, 0.15, and 0.29 at the 16-day scale, respectively.

Spatial patterns of habitat use related to vegetation productivity were also unexpected (Fig. 6). Annual counts of detections were not always positively associated with vegetation productivity, nor did they increase more with CT metrics than with satellite metrics. While caribou and deer detections were greater at sites with greater maximum greenness measured by CTs ($\beta_{maxCT\_caribou} = 0.17 \pm 0.08$, $P = 0.02$; $\beta_{maxCT\_deer} = 0.29 \pm 0.08$, $P < 0.01$), crane and deer detections respectively were fewer at sites with greater cumulative greenness measured by CTs ($\beta_{cumCT\_crane} = -0.26 \pm 0.06$, $P < 0.01$) and maximum greenness measured by EVI ($\beta_{maxEVI\_deer} = -0.19 \pm 0.10$, $P = 0.05$). Cumulative greenness measured only by NDVI was a top predictor for the annual count of deer detections at a site ($\beta_{cumNDVI\_deer} = 0.36 \pm 0.13$; $P < 0.01$). Length of growing season measured by CTs, seasonality of NDVI and EVI, and cumulative EVI had no support in initial models for any species and were excluded from subsequent consideration. Final annual models for cranes, caribou, and deer had high explanatory

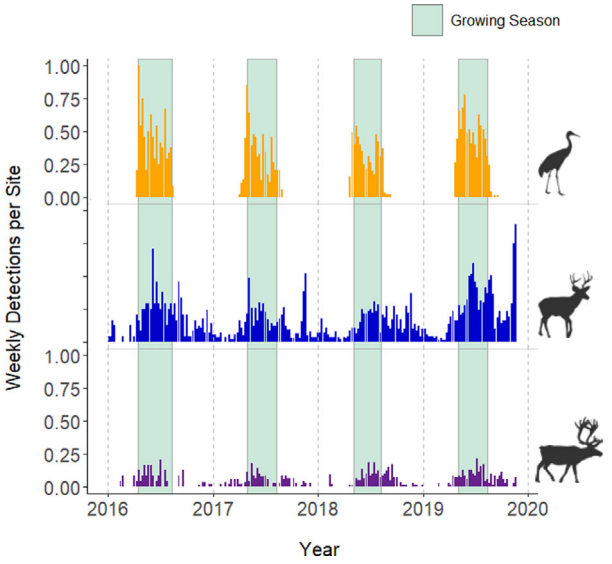

Figure 4. Number of independent detections per week per site of sandhill crane, woodland caribou, and white-tailed deer at n = 73 camera trap (CT) sites across sampling strata in the study area in northern Alberta, Canada from January 2016 to November 2019. Independent detections were identified based on a 30 min maximum threshold for images to be considered part of the same detection event. Background rectangles show the vegetation growing season estimated from the extracted dates of understory green-up to senescence using CT time-lapse images.

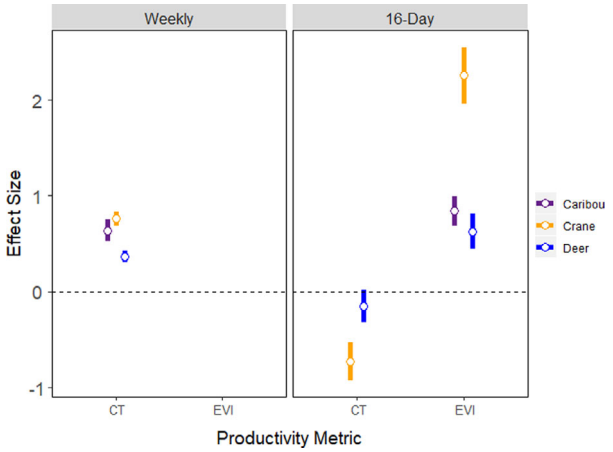

Figure 5. Estimated effect sizes of top vegetation productivity (greenness) predictors in models of weekly and 16-day counts of detections for sandhill crane, woodland caribou, and white-tailed deer per site at n = 73 camera trap (CT) sites within the study area in northern Alberta Canada, from January 2016 to November 2019. Mean estimates with 95% confidence intervals are shown. Results are from generalized linear mixed models with year and camera trap as random intercepts and (log) number of days of CT operation as an offset.

power, with Ω^2 statistics of 0.93, 0.85, and 0.86, respectively.

Discussion

Understanding the linkages between wildlife and their habitat is critical for biodiversity conservation in the face of global landscape change. Our findings establish the ability of CTs to detect vegetation patterns based on automated extraction of greenness using an *a priori* approach with standardized time-lapse sampling, building on *post hoc* analyses with "by-catch" vegetation data. Importantly, CTs revealed vegetation dynamics that differed markedly from those derived from satellite data, and suggested new patterns of wildlife habitat use related to vegetation productivity. CTs detected slow and ongoing understory vegetation recovery but also evidence of persistent habitat disturbance from petroleum exploration despite restoration efforts, highlighting the importance of long-term monitoring with a diverse set of metrics and indicators of habitat condition.

Discrepancies between satellite and CT metrics (Fig. 2) may have been partially due to differences in spatiotemporal resolution. MODIS satellite data were collected as infrequently as every 16 days and at lower spatial resolution (30–250 m) than the size of 8-m-wide seismic lines, while CTs captured vegetation patterns every day at this higher spatial resolution. CT and satellite metrics provided similar but different signals of vegetation productivity even when greenness from CTs was grouped to match the 16-day resolution and dates of the MODIS-derived NDVI and EVI (Fig. S7), consistent with other research demonstrating that the relationship between local greenness measured by digital imagery and gross primary productivity is site specific (Westergaard-Nielsen et al., 2017). Thus, CTs are a valuable tool for investigating local vegetation dynamics. Furthermore, differences in spatial resolution necessarily resulted in satellites capturing canopy signals beyond the 8-m width of seismic lines, and may have been compounded by vertical habitat structure and overhead angles of satellites that would have blocked understory vegetation from view and led to poor detection of the understory (Borowik et al., 2013; Fortin et al., 2019; Liu et al., 2017). Such physical obstruction can be especially problematic in boreal landscapes with snow cover and coniferous canopies (Karkauskaite et al., 2017; Yun et al., 2018). Even within satellite measures (Figs. 2 and 6), observed differences underscore the consequences of choosing appropriate metrics and scales of inference in heterogeneous landscapes (Dronova et al., 2021). Our findings are consistent with known discrepancies between satellite and ground-level sensing of understory vegetation patterns (McClelland et al., 2019;

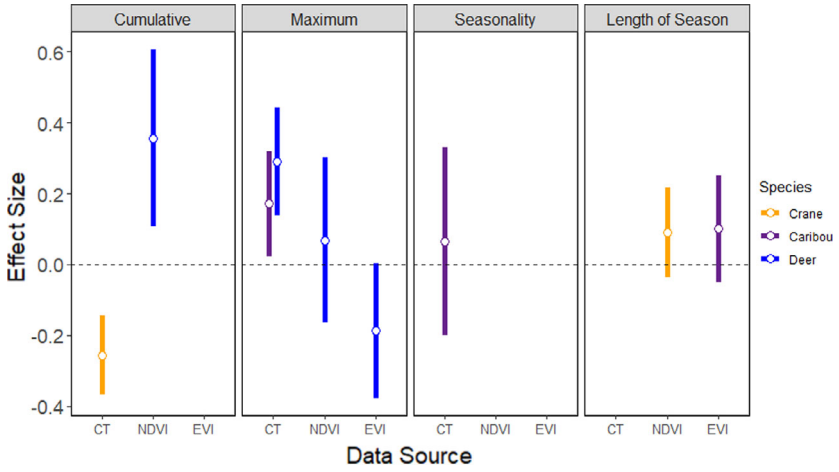

Figure 6. Estimated effect sizes of top vegetation productivity predictors in final models of annual counts of detections for sandhill crane, woodland caribou, and white-tailed deer per site at n = 73 camera trap (CT) sites in the study area in northern Alberta, Canada, from January 2016 to November 2019. Cumulative greenness is the area under each annual greenness curve; maximum greenness is the peak value during each annual cycle; seasonality is the coefficient of variation across daily values; length of growing season (LOS) is the annual difference in days between green-up and senescence. Mean estimates with 95% confidence intervals are shown. Results are from generalized linear mixed models with year and CT site as random intercepts and (log) number of days of CT operation as an offset.

Tuanmu et al., 2010; Zhao et al., 2020), but also demonstrate a way forward through CTs to acknowledge these differences when making ecological inferences.

Our CTs detected differences in understory phenology and productivity patterns across sampling strata, with some evidence that vegetation regeneration has been occurring on seismic lines due to restoration treatment. Topography (i.e., elevation, slope, aspect) was similar across sites (Table 2), and thus likely was not responsible for the range of observed vegetation differences. However, seismic line orientation can influence microclimate conditions and potentially also vegetation (Franklin et al. 2021). As such, the significant variation in senescence dates across years at only sites that received restoration treatments (Active and Passive sites) could be due to plant succession with higher species turnover typical of annual species. Our findings lay the foundation and motivation for future research to identify the particular plant species and plant compositions contributing to observed patterns within and across sampling strata – either through manual identification (Vartanian et al. 2014, Hofmeester et al. 2019) or automated approaches based on machine learning (Rzanny et al. 2019; Tabak et al., 2019; Wäldchen & Mäder, 2018). Identifying plant species in CT images could provide insight into how various disturbances such as seismic lines, forest harvest practices, forest fires, and climate change differentially impact local vegetation dynamics and their links to wildlife foraging. Thus, CTs can play an important role in relating habitat change to specific vegetation dynamics.

Monitoring restoration effectiveness in this landscape is important due to its role in caribou conservation, as vegetation growth on seismic lines is expected to help restore altered interactions between threatened caribou and their competitors and predators. Restoring vegetation patterns to undisturbed conditions should reduce forage subsidies that attract apparent competitors such as deer, and impede movement of predators including wolves and bears (Dickie et al., 2017, 2019; McKenzie et al., 2012). Despite some differences, many similarities remained across sites on seismic lines. Thus, given that regeneration of herbaceous and woody materials can take decades in disturbed boreal landscapes (van Rensen et al., 2015) and restoration began ≤8 years prior to this study, continued assessment of response to restoration treatments and further vegetation recovery through either passive or recurrent active restoration efforts (Finnegan et al., 2018) will be necessary to achieve vegetation functions and wildlife interactions consistent with natural boreal conditions.

Uniquely, understory vegetation dynamics measured from CTs contributed to inferences about wildlife habitat use not possible with only satellite metrics. Caribou and deer use increased with weekly and annual maximum understory greenness, consistent with their tracking of temporal and spatial patterns of understory food resources, including deciduous shrubs, soft mast, and other seral vegetation (Dawe et al., 2017; Denryter et al., 2017). The unexpected weaker effect of understory greenness on weekly and 16-day counts for deer compared with caribou (Fig. 5) may be due to differences in forage preference and

movement patterns, and highlights additional research opportunities to identify the mechanisms underlying the observed relative effect sizes. Deer have lower forage selectivity and higher rates of daily summer movement (Crête et al., 2001; Ferguson & Elkie, 2004; Webb et al., 2010), which would have supported foraging at more sites with less understory productivity. Indeed, deer were detected at 18 (25%) more sites than caribou (n = 59 vs. n = 41). Identifying plant species in CT images could elucidate if deer, which have been rarely studied at the northern limit of their expanding range (Fisher & Burton, 2018; Laurent et al. 2021), were foraging on a greater diversity of species or selecting more commonly distributed species. Also, seasonal differences in movement dynamics related not just to vegetation but also timing of parturition and other life-history strategies (Ferguson & Elkie, 2004) likely contributed to the stronger effect of greenness on caribou and could be further investigated. Un-modeled factors contributing to cranes, including soil conditions that affect prey availability in the understory (Davis et al., 2006; Mullins & Bizeau, 1978), may have contributed to the low explanatory power of weekly and 16-day count models and explain why crane counts were not always greater in areas of higher vegetation productivity (Fig. 6). Notably, wildlife habitat use varied with spatiotemporal scale (McNeill et al., 2020), indicated by the positive associations between weekly counts exclusively with understory greenness and 16-day counts exclusively with EVI (Fig. 5). Wildlife were likely tracking understory vegetation at shorter time scales due to faster changes in understory resources, compared with canopy changes. Considering only satellite-based metrics, canopy productivity would have failed to detect these understory and scale-specific patterns.

Detection probability of animals around CT sites was undoubtedly imperfect, with wildlife using areas adjacent to the relatively small CT zone of detection. However, individuals of the three focal species were unlikely to be missed when passing in front of the CT due to their fairly large body sizes, camera placement, and relatively low vegetation height (Fig. S3). Also, independent detection events were less likely to miss all instances of individuals passing by within a 30 min period, as cranes, deer, and caribou respectively had independent detection events composed of an average 5, 9, and 10 CT images. For smaller species, imperfect and variable detection probability could render detections an unreliable relative measure of habitat use, and motivate a modeling approach that may better account for detectability (McKenzie et al., 2012, Burton et al. 2015; but see Neilson et al. 2018 and Stewart et al. 2018 for discussions of the limitations of applying occupancy models to CT surveys). Perhaps more subtly, imperfect detection due to individuals using similar habitat adjacent to the CT detection zone could have led to biased site-specific estimates and imprecise across-site estimates of concordance between focal species and vegetation phenology. However, accounting for imperfect detection would not have changed our inferences. Even with imperfect detection, deer and caribou were already detected throughout the year and the concordance across sites between crane detections, and the growing season was not so imprecise as to result in statistical differences. Furthermore, given that all focal species were detected in all sampling strata and habitat types, there was no reason to expect systematic biases in detection probability or patterns of movement around CTs that would have warranted alternative approaches to estimating concordance between vegetation phenology and wildlife habitat use (e.g., Roth et al. 2014).

Our results highlight the need for a diverse set of vegetation and wildlife tools to monitor landscape change and biodiversity responses. In addition to general patterns of vegetation phenology and productivity, CTs may also be used to identify plant species, focusing on specific ones (Vartanian et al. 2014), and to measure the abundance or intensity of phenological stages such as flowering or fruiting (Denny et al., 2014; Hofmeester et al. 2019; Vartanian et al., 2014). Satellite data that pre-date CT monitoring may help determine longer-term trends and historical habitat baselines. Satellite data also provide spatially continuous habitat data useful for predictions – an advantage over CTs, which provide data at point locations with an unclear effective sampling area beyond the immediate field of view (Foster & Harmsen, 2012). Ultimately, monitoring habitat changes should consider intra- and interspecific biotic interactions as these reflect underlying ecological processes and ecosystem function (Lomov et al., 2009; Torre Cerro & Holloway, 2020). Indeed, observed differences in understory dynamics between sampling strata in our study area have not been associated with noticeable wildlife recovery – caribou, their predators, and competitors have all continued to use seismic lines (Tattersall et al., 2020a,b). The return of species interactions to pre-seismic line conditions is therefore ongoing. We recommend long-term, multimethod approaches that monitor both vegetation dynamics and wildlife habitat use (Miller & Hobbs, 2007; Taddeo & Dronova, 2018; Wagner et al., 2008).

Coordinated, long-term monitoring of wildlife and the resources they rely on is important for building a mechanistic understanding of how species track resources and interact with changing environments (Campeau et al., 2019). CTs promise to be a valuable and cost-effective tool in this endeavor (Steenweg et al., 2017), with novel lines of inquiry and methodologies in development. For example, in addition to vegetation signals measured from the greenness values in CT images, the red, blue, and even

brightness values may be informative about wildfire and snow regimes; both affect wildlife habitat use (Fisher et al., 2020; Fisher & Wilkinson, 2005; Serbin et al., 2009) and are shifting due to climate change (Hansen et al., 2011; Price et al., 2013). Careful sampling design will help capture environmental signals of interest and move CT surveys away from *post hoc* analyses of by-catch vegetation data, while automated extraction can help scale up such efforts. Another promising line of research is the development of integrated canopy and understory metrics, such as with satellites and CTs, to characterize habitat conditions across spatiotemporal scales (e.g., Baumann et al., 2017; McClelland et al., 2019). In the face of increasing habitat disturbance in the Anthropocene and the need for effective wildlife conservation, we strongly advocate for the use of long-term camera trapping surveys in disturbed landscapes to investigate wildlife and habitat patterns to understand the processes underlying ecological interactions and habitat change.

Acknowledgments

We thank R. Harding (CNOOC Petroleum North America), R. Albricht and S. Grindal (ConocoPhillips), M. Boulton (Suncor), J. Gareau (Canadian Natural Resources Ltd), J. Peters (Silvacom), and B. Eaton (InnoTech) for support. E. Tattersall, L. Nolan, A. Underwood, S. Frey, and B. Sarchuk assisted with field data collection, and T. Justason provided initial assistance with phenology data processing. This work was funded by oil sands operators involved in the Algar Caribou Habitat Restoration Program, with additional funding from the Alberta Upstream Petroleum Research Fund, Innotech Alberta, the University of British Columbia, Canada Research Chairs Program, Natural Sciences and Engineering Research Council of Canada, Northern Scientific Training Program, and Mitacs.

Conflict of Interest

We declare no conflicts of interest.

Data Availability Statement

Data analysis scripts will be made available upon manuscript acceptance on the corresponding author's public Github.

References

Alberton, B., Torres, R.d.S., Cancian, L.F., Borges, B.D., Almeida, J., Mariano, G.C. et al. (2017) Introducing digital cameras to monitor plant phenology in the tropics: applications for conservation. *Perspectives in Ecology and Conservation*, **15**, 82–90. https://doi.org/10.1016/j.pecon.2017.06.004

Ancin-Murguzur, F.J., Munoz, L., Monz, C. & Hausner, V.H. (2020) Drones as a tool to monitor human impacts and vegetation changes in parks and protected areas. *Remote Sensing in Ecology and Conservation*, **6**, 105–113. https://doi.org/10.1002/rse2.127

Armstrong, J.B., Takimoto, G., Schindler, D.E., Hayes, M.M. & Kauffman, M.J. (2016) Resource waves: phenological diversity enhances foraging opportunities for mobile consumers. *Ecology*, **97**, 1099–1112. https://doi.org/10.1890/15-0554.1

Barton, K. (2020) *MuMIn: multi-model inference*. R package version 1.43.17.

Bater, C.W., Coops, N.C., Wulder, M.A., Nielsen, S.E., McDermid, G. & Stenhouse, G.B. (2011) Design and installation of a camera network across an elevation gradient for habitat assessment. *Instrumentation Science & Technology*, **39**, 231–247. https://doi.org/10.1080/10739149.2011.564700

Baumann, M., Ozdogan, M., Richardson, A.D. & Radeloff, V.C. (2017) Phenology from Landsat when data is scarce: using MODIS and Dynamic Time-Warping to combine multi-year Landsat imagery to derive annual phenology curves. *International Journal of Applied Earth Observation and Geoinformation*, **54**, 72–83. https://doi.org/10.1016/j.jag.2016.09.005

Bolton, D.K., Gray, J.M., Melaas, E.K., Moon, M., Eklundh, L. & Friedl, M.A. (2020) Continental-scale land surface phenology from harmonized Landsat 8 and Sentinel-2 imagery. *Remote Sensing of Environment*, **240**, 111685. https://doi.org/10.1016/j.rse.2020.111685

Borowik, T., Pettorelli, N., Sönnichsen, L. & Jędrzejewska, B. (2013) Normalized difference vegetation index (NDVI) as a predictor of forage availability for ungulates in forest and field habitats. *European Journal of Wildlife Research*, **59**, 675–682. https://doi.org/10.1007/s10344-013-0720-0

Bradshaw, C.J.A., Warkentin, I.G. & Sodhi, N.S. (2009) Urgent preservation of boreal carbon stocks and biodiversity. *Trends in Ecology & Evolution*, **24**, 541–548. https://doi.org/10.1016/j.tree.2009.03.019

Brooks, M., Kristensen, K., Benthem, K., Magnusson, A., Berg, C., Nielsen, A. et al. (2017) glmmTMB balances speed and flexibility among packages for zero-inflated generalized linear mixed modeling. *The R Journal*, **9**(2), 378–400.

Buisson, E., Alvarado, S.T., Stradic, S.L. & Morellato, L.P.C. (2017) Plant phenological research enhances ecological restoration. *Restoration Ecology*, **25**, 164–171. https://doi.org/10.1111/rec.12471

Burton, A.C., Neilson, E., Moreira, D., Ladle, A., Steenweg, R., Fisher, J.T. et al. (2015) Wildlife camera trapping: a review and recommendations for linking surveys to ecological processes. *Journal of Applied Ecology*, **52**, 675–685. https://doi.org/10.1111/1365-2664.12432

Burton, C., Burgar, J., Tattersall, E. & Fisher, J. (2017) *Algar Wildlife Monitoring Project: 2017 Annual Progress Report*. University of British Columbia and InnoTech Alberta.

Campeau, A.B., Rickbeil, G.J.M., Coops, N.C. & Côté, S.D. (2019) Long-term changes in the primary productivity of migratory caribou (*Rangifer tarandus*) calving grounds and summer pasture on the Quebec-Labrador Peninsula (Northeastern Canada): the mixed influences of climate change and caribou herbivory. *Polar Biology*, **42**, 1005–1023. https://doi.org/10.1007/s00300-019-02492-6

Canada, Environment Canada. (2015) *Recovery strategy for the Woodland Caribou (Rangifer tarandus caribou)*, boreal population, in Canada.

Connell, J.H. & Slatyer, R.O. (1977) Mechanisms of succession in natural communities and their role in community stability and organization. *The American Naturalist*, **111**, 1119–1144. https://doi.org/10.1086/283241

Coops, N.C., Wulder, M.A., Duro, D.C., Han, T. & Berry, S. (2008) The development of a Canadian dynamic habitat index using multi-temporal satellite estimates of canopy light absorbance. *Ecological Indicators*, **8**, 754–766. https://doi.org/10.1016/j.ecolind.2008.01.007

Crête, M., Ouellet, J.-P. & Lesage, L. (2001) Comparative effects on plants of caribou/reindeer, moose and white-tailed deer herbivory. *Arctic*, **54**, 407–417.

Dabros, A., Pyper, M. & Castilla, G. (2018) Seismic lines in the boreal and arctic ecosystems of North America: environmental impacts, challenges, and opportunities. *Environmental Reviews*, **26**, 214–229. https://doi.org/10.1139/er-2017-0080

Davis, C.A., Austin, J.E. & Buhl, D.A. (2006) Factors influencing soil invertebrate communities in riparian grasslands of the central Platte River floodplain. *Wetlands*, **26**, 438–454. https://doi.org/10.1672/0277-5212(2006)26[438:FISICI]2.0.CO;2

Dawe, C.A., Filicetti, A.T. & Nielsen, S.E. (2017) Effects of linear disturbances and fire severity on velvet leaf blueberry abundance, vigor, and berry production in recently burned jack pine forests. *Forests*, **8**, 398. https://doi.org/10.3390/f8100398

Dawe, K.L., Bayne, E.M. & Boutin, S. (2014) Influence of climate and human land use on the distribution of white-tailed deer (*Odocoileus virginianus*) in the western boreal forest. *Canadian Journal of Zoology*, **92**, 353–363. https://doi.org/10.1139/cjz-2013-0262

Denny, E.G., Gerst, K.L., Miller-Rushing, A.J., Tierney, G.L., Crimmins, T.M., Enquist, C.A.F. et al. (2014) Standardized phenology monitoring methods to track plant and animal activity for science and resource management applications. *International Journal of Biometeorology*, **58**(4), 591–601.

Denryter, K.A., Cook, R.C., Cook, J.G. & Parker, K.L. (2017) Straight from the caribou's (*Rangifer tarandus*) mouth: detailed observations of tame caribou reveal new insights into summer–autumn diets. *Canadian Journal of Zoology*, **95**, 81–94. https://doi.org/10.1139/cjz-2016-0114

Dickie, M., McNay, S.R., Sutherland, G.D., Cody, M. & Avgar, T. (2019) Corridors or risk? Movement along, and use of, linear features varies predictably among large mammal predator and prey species. *Journal of Animal Ecology*, **89**(2), 623–634. https://doi.org/10.1111/1365-2656.13130

Dickie, M., Serrouya, R., McNay, R.S. & Boutin, S. (2017) Faster and farther: wolf movement on linear features and implications for hunting behaviour. *Journal of Applied Ecology*, **54**, 253–263. https://doi.org/10.1111/1365-2664.12732

Didan, K. (2015) *MOD13Q1 MODIS/terra vegetation indices 16-day L3 global 250m SIN grid. NASA LP DAAC*. https://doi.org/10.5067/MODIS/MOD13Q1.006

Doyle, T., Hawkes, W.L.S., Massy, R., Powney, G.D., Menz, M.H.M. & Wotton, K.R. (2020) Pollination by hoverflies in the Anthropocene. *Proceedings of the Royal Society B: Biological Sciences*, **287**, 20200508. https://doi.org/10.1098/rspb.2020.0508

Dronova, I., Taddeo, S., Hemes, K.S., Knox, S.H., Valach, A., Oikawa, P.Y. et al. (2021) Remotely sensed phenological heterogeneity of restored wetlands: linking vegetation structure and function. *Agricultural and Forest Meteorology*, **296**, 108215. https://doi.org/10.1016/j.agrformet.2020.108215

Emmett, K.D., Renwick, K.M. & Poulter, B. (2019) Disentangling climate and disturbance effects on regional vegetation greening trends. *Ecosystems*, **22**, 873–891. https://doi.org/10.1007/s10021-018-0309-2

Ferguson, S.H. & Elkie, P.C. (2004) Seasonal movement patterns of woodland caribou (*Rangifer tarandus caribou*). *Journal of Zoology*, **262**, 125–134. https://doi.org/10.1017/S0952836903004552

Filicetti, A.T., Cody, M. & Nielsen, S.E. (2019) Caribou conservation: restoring trees on seismic lines in Alberta, Canada. *Forests*, **10**, 185. https://doi.org/10.3390/f10020185

Filippa, G., Cremonese, E., Migliavacca, M., Galvagno, M., Forkel, M., Wingate, L. et al. (2016) Phenopix: a R package for image-based vegetation phenology. *Agricultural and Forest Meteorology*, **220**, 141–150. https://doi.org/10.1016/j.agrformet.2016.01.006

Finnegan, L., MacNearney, D. & Pigeon, K.E. (2018) Divergent patterns of understory forage growth after seismic line exploration: implications for caribou habitat restoration. *Forest Ecology and Management*, **409**, 634–652. https://doi.org/10.1016/j.foreco.2017.12.010

Finnegan, L., Pigeon, K.E. & MacNearney, D. (2019) Predicting patterns of vegetation recovery on seismic lines: informing restoration based on understory species composition and growth. *Forest Ecology and Management*, **446**, 175–192. https://doi.org/10.1016/j.foreco.2019.05.026

Fisher, J.T. & Burton, A.C. (2018) Wildlife winners and losers in an oil sands landscape. *Frontiers in Ecology and the Environment*, **16**, 323–328. https://doi.org/10.1002/fee.1807

Fisher, J.T., Burton, A.C., Nolan, L. & Roy, L. (2020) Influences of landscape change and winter severity on invasive ungulate persistence in the Nearctic boreal forest. *Scientific Reports*, **10**, 8742. https://doi.org/10.1038/s41598-020-65385-3

Fisher, J.T. & Wilkinson, L. (2005) The response of mammals to forest fire and timber harvest in the North American boreal forest. *Mammal Review*, **35**, 51–81. https://doi.org/10.1111/j.1365-2907.2005.00053.x

Fortin, J.A., Fisher, J.T., Rhemtulla, J.M. & Higgs, E.S. (2019) Estimates of landscape composition from terrestrial oblique photographs suggest homogenization of Rocky Mountain landscapes over the last century. *Remote Sens Ecol Conserv*, **5**, 224–236. https://doi.org/10.1002/rse2.100

Foster, R.J. & Harmsen, B.J. (2012) A critique of density estimation from camera-trap data. *The Journal of Wildlife Management*, **76**, 224–236. https://doi.org/10.1002/jwmg.275

Franklin, C.M.A., Filicetti, A.T. & Nielsen, S.E. (2021) Seismic line width and orientation influence microclimatic forest edge gradients and tree regeneration. *Forest Ecology and Management*, **492**, 119216. https://doi.org/10.1016/j.foreco.2021.119216

Gann, G.D., McDonald, T., Walder, B., Aronson, J., Nelson, C.R., Jonson, J. et al. (2019) International principles and standards for the practice of ecological restoration. Second edition. *Restoration Ecology*, **27**, S1–S46. https://doi.org/10.1111/rec.13035

Gentry, A.H. & Emmons, L.H. (1987) Geographical variation in fertility, phenology, and composition of the understory of neotropical forests. *Biotropica*, **19**, 216–227. https://doi.org/10.2307/2388339

Hansen, B.B., Aanes, R., Herfindal, I., Kohler, J. & Sæther, B.-E. (2011) Climate, icing, and wild arctic reindeer: past relationships and future prospects. *Ecology*, **92**, 1917–1923. https://doi.org/10.1890/11-0095.1

Hebblewhite, M. (2017) Billion dollar boreal woodland caribou and the biodiversity impacts of the global oil and gas industry. *Biological Conservation*, **206**, 102–111. https://doi.org/10.1016/j.biocon.2016.12.014

Hendry, H. & Mann, C. (2018) Camelot—intuitive software for camera-trap data management. *Oryx*, **52**, 15. https://doi.org/10.1017/S0030605317001818

Hervieux, D., Hebblewhite, M., DeCesare, N.J., Russell, M., Smith, K., Robertson, S. et al. (2013) Widespread declines in woodland caribou (*Rangifer tarandus caribou*) continue in Alberta. *Canadian Journal of Zoology*, **91**, 872–882. https://doi.org/10.1139/cjz-2013-0123

Hobi, M.L., Dubinin, M., Graham, C.H., Coops, N.C., Clayton, M.K., Pidgeon, A.M. et al. (2017) A comparison of Dynamic Habitat Indices derived from different MODIS products as predictors of avian species richness. *Remote Sensing of Environment*, **195**, 142–152. https://doi.org/10.1016/j.rse.2017.04.018

Hobson, K.A., Wilgenburg, S.V., Wassenaar, L.I., Hands, H., Johnson, W.P., O'Meilia, M. et al. (2006) Using stable hydrogen isotope analysis of feathers to delineate origins of harvested sandhill cranes in the Central Flyway of North America. *Waterbirds*, **29**, 137–147. https://doi.org/10.1675/1524-4695(2006)29[137:USHIAO]2.0.CO;2

Hofmeester, T.R., Young, S., Juthberg, S., Singh, N.J., Widemo, F., Andrén, H. et al. (2019) Using by-catch data from wildlife surveys to quantify climatic parameters and the timing of phenology for plants and animals using camera traps. *Remote Sensing in Ecology and Conservation*, **6**, 129–140. https://doi.org/10.1002/rse2.136

Ide, R. & Oguma, H. (2010) Use of digital cameras for phenological observations. *Ecological Informatics*, **5**, 339–347. https://doi.org/10.1016/j.ecoinf.2010.07.002

Iversen, M., Fauchald, P., Langeland, K., Ims, R.A., Yoccoz, N.G. & Bråthen, K.A. (2014) Phenology and cover of plant growth forms predict herbivore habitat selection in a high latitude ecosystem. *PLoS One*, **9**, e100780. https://doi.org/10.1371/journal.pone.0100780

Jiang, Z., Huete, A.R., Didan, K. & Miura, T. (2008) Development of a two-band enhanced vegetation index without a blue band. *Remote Sensing of Environment*, **112**, 3833–3845. https://doi.org/10.1016/j.rse.2008.06.006

Karkauskaite, P., Tagesson, T. & Fensholt, R. (2017) Evaluation of the Plant Phenology Index (PPI), NDVI and EVI for start-of-season trend analysis of the northern hemisphere boreal zone. *Remote Sensing*, **9**, 485. https://doi.org/10.3390/rs9050485

Latham, A.D.M., Latham, M.C., Mccutchen, N.A. & Boutin, S. (2011) Invading white-tailed deer change wolf–caribou dynamics in northeastern Alberta. *The Journal of Wildlife Management*, **75**, 204–212. https://doi.org/10.1002/jwmg.28

Laurent, M., Dickie, M., Becker, M., Serrouya, R. & Boutin, S. (2021) Evaluating the mechanisms of landscape change on white-tailed deer populations. *The Journal of Wildlife Management*, **85**, 340–353. https://doi.org/10.1002/jwmg.21979

Lee, P. & Boutin, S. (2006) Persistence and developmental transition of wide seismic lines in the western Boreal Plains of Canada. *Journal of Environmental Management*, **78**, 240–250. https://doi.org/10.1016/j.jenvman.2005.03.016

Lewis, S.L. & Maslin, M.A. (2015) Defining the anthropocene. *Nature*, **519**, 171–180. https://doi.org/10.1038/nature14258

Liu, Y., Hill, M.J., Zhang, X., Wang, Z., Richardson, A.D., Hufkens, K. et al. (2017) Using data from Landsat, MODIS, VIIRS and PhenoCams to monitor the phenology of California oak/grass savanna and open grassland across spatial scales. *Agricultural and Forest Meteorology*, **237–238**, 311–325. https://doi.org/10.1016/j.agrformet.2017.02.026

Lomov, B., Keith, D.A. & Hochuli, D.F. (2009) Linking ecological function to species composition in ecological restoration: seed removal by ants in recreated woodland.

Austral Ecology, **34**, 751–760. https://doi.org/10.1111/j.1442-9993.2009.01981.x

Lone, K., van Beest, F.M., Mysterud, A., Gobakken, T., Milner, J.M., Ruud, H.-P. et al. (2014) Improving broad scale forage mapping and habitat selection analyses with airborne laser scanning: the case of moose. *Ecosphere*, **5**, art144. https://doi.org/10.1890/ES14-00156.1

Lopatin, J., Dolos, K., Kattenborn, T. & Fassnacht, F.E. (2019) How canopy shadow affects invasive plant species classification in high spatial resolution remote sensing. *Remote Sensing in Ecology and Conservation*, **5**, 302–317. https://doi.org/10.1002/rse2.109

Lupardus, R.C., McIntosh, A.C.S., Janz, A. & Farr, D. (2019) Succession after reclamation: identifying and assessing ecological indicators of forest recovery on reclaimed oil and natural gas well pads. *Ecological Indicators*, **106**, 105515. https://doi.org/10.1016/j.ecolind.2019.105515

Mahon, C.L., Holloway, G.L., Bayne, E.M. & Toms, J.D. (2019) Additive and interactive cumulative effects on boreal landbirds: winners and losers in a multi-stressor landscape. *Ecological Applications*, **29**, e01895. https://doi.org/10.1002/eap.1895

Mazerolle, M.J. (2019). *AICcmodavg: model selection and multimodel inference based on (Q)AIC(c)*. R package version 2.2-2. https://cran.r-project.org/package=AICcmodavg

McClelland, C.J.R., Coops, N.C., Berman, E.E., Kearney, S.P., Nielsen, S.E., Burton, A.C. et al. (2019) Detecting changes in understorey and canopy vegetation cycles in West Central Alberta using a fusion of Landsat and MODIS. *Applied Vegetation Science*, **23**(2), 223–238. https://doi.org/10.1111/avsc.12466

McKenzie, H.W., Merrill, E.H., Spiteri, R.J. & Lewis, M.A. (2012) How linear features alter predator movement and the functional response. *Interface Focus*, **2**, 205–216. https://doi.org/10.1098/rsfs.2011.0086

McNeill, E.P., Thompson, I.D., Wiebe, P.A., Street, G.M., Shuter, J., Rodgers, A.R. et al. (2020) Multi-scale foraging decisions made by woodland caribou (*Rangifer tarandus caribou*) in summer. *Canadian Journal of Zoology*, **98**, 331–341. https://doi.org/10.1139/cjz-2019-0197

Merkle, J.A., Monteith, K.L., Aikens, E.O., Hayes, M.M., Hersey, K.R., Middleton, A.D. et al. (2016) Large herbivores surf waves of green-up during spring. *Proceedings of the Royal Society B: Biological Sciences*, **283**, 20160456. https://doi.org/10.1098/rspb.2016.0456

Miller, J.R. & Hobbs, R.J. (2007) Habitat restoration—do we know what we're doing? *Restoration Ecology*, **15**, 382–390. https://doi.org/10.1111/j.1526-100X.2007.00234.x

Mills, L.S., Bragina, E.V., Kumar, A.V., Zimova, M., Lafferty, D.J.R., Feltner, J. et al. (2018) Winter color polymorphisms identify global hot spots for evolutionary rescue from climate change. *Science*, **359**, 1033–1036. https://doi.org/10.1126/science.aan8097

Moore, C.E., Brown, T., Keenan, T.F., Duursma, R.A., van Dijk, A.I.J.M., Beringer, J. et al. (2016) Reviews and syntheses: Australian vegetation phenology: new insights from satellite remote sensing and digital repeat photography. *Biogeosciences*, **13**, 5085–5102. https://doi.org/10.5194/bg-13-5085-2016

Morellato, L.P.C., Alberton, B., Alvarado, S.T., Borges, B., Buisson, E., Camargo, M.G.G. et al. (2016) Linking plant phenology to conservation biology. *Biological Conservation*, **195**, 60–72. https://doi.org/10.1016/j.biocon.2015.12.033

Mueller, T., Olson, K.A., Fuller, T.K., Schaller, G.B., Murray, M.G. & Leimgruber, P. (2008) In search of forage: predicting dynamic habitats of Mongolian gazelles using satellite-based estimates of vegetation productivity. *Journal of Applied Ecology*, **45**, 649–658. https://doi.org/10.1111/j.1365-2664.2007.01371.x

Mullins, W.H. & Bizeau, E.G. (1978) Summer foods of sandhill cranes in Idaho. *The Auk*, **95**, 175–178. https://doi.org/10.2307/4085509

Neilson, E.W., Avgar, T., Burton, A.C., Broadley, K. & Boutin, S. (2018) Animal movement affects interpretation of occupancy models from camera-trap surveys of unmarked animals. *Ecosphere*, **9**, 1–15. https://doi.org/10.1002/ecs2.2092

Nexen and Silvacom. (2015) *Algar caribou habitat restoration program 2014/15*. Unpublished Report.

Pauley, G.R., Peek, J.M. & Zager, P. (1993) Predicting white-tailed deer habitat use in Northern Idaho. *The Journal of Wildlife Management*, **57**, 904–913. https://doi.org/10.2307/3809096

Pickell, P.D., Andison, D.W., Coops, N.C., Gergel, S.E. & Marshall, P.L. (2015) The spatial patterns of anthropogenic disturbance in the western Canadian boreal forest following oil and gas development. *Canadian Journal of Forest Research*, **45**, 732–743. https://doi.org/10.1139/cjfr-2014-0546

Price, D.T., Alfaro, R.I., Brown, K.J., Flannigan, M.D., Fleming, R.A., Hogg, E.H. et al. (2013) Anticipating the consequences of climate change for Canada's boreal forest ecosystems. *Environmental Reviews*, **21**, 322–365. https://doi.org/10.1139/er-2013-0042

R Core Team. (2019) *R: a language and environment for statistical computing*. Vienna, Austria: R Foundation for Statistical Computing. https://www.R-project.org/.

Radeloff, V.C., Dubinin, M., Coops, N.C., Allen, A.M., Brooks, T.M., Clayton, M.K. et al. (2019) The Dynamic Habitat Indices (DHIs) from MODIS and global biodiversity. *Remote Sensing of Environment*, **222**, 204–214. https://doi.org/10.1016/j.rse.2018.12.009

Razenkova, E., Radeloff, V.C., Dubinin, M., Bragina, E.V., Allen, A.M., Clayton, M.K. et al. (2020) Vegetation productivity summarized by the Dynamic Habitat Indices explains broad-scale patterns of moose abundance across Russia. *Scientific Reports*, **10**, 836. https://doi.org/10.1038/s41598-019-57308-8

Rettie, W.J. & Messier, F. (2001) Range use and movement rates of woodland caribou in Saskatchewan. *Canadian Journal of Zoology*, **79**, 1933–1940. https://doi.org/10.1139/z01-156

Richardson, A.D. & O'Keefe, J. (2009) Phenological differences between understory and overstory. In: Noormets, A. (Ed.) *Phenology of ecosystem processes: applications in global change research*. New York, NY: Springer, pp. 87–117. https://doi.org/10.1007/978-1-4419-0026-5_4

Robinne, F.N., Parisien, M.A. & Flannigan, M. (2016) Anthropogenic influence on wildfire activity in Alberta, Canada. *International Journal of Wildland Fire*,, **25**, 1131. https://doi.org/10.1071/WF16058

Roth, T., Strebel, N. & Amrhein, V. (2014) Estimating unbiased phenological trends by adapting site-occupancy models. *Ecology*, **95**, 2144–2154. https://doi.org/10.1890/13-1830.1

Rovero, F. & Zimmermann, F. (2016) *Camera trapping for wildlife research*. Exeter: Pelagic Publishing Ltd.

Rzanny, M., Mäder, P., Deggelmann, A., Chen, M. & Wäldchen, J. (2019) Flowers, leaves or both? How to obtain suitable images for automated plant identification. *Plant Methods*, **15**, 77. https://doi.org/10.1186/s13007-019-0462-4

Sakai, S. & Kitajima, K. (2019) Tropical phenology: recent advances and perspectives. *Ecological Research*, **34**, 50–54. https://doi.org/10.1111/1440-1703.1131

Sankey, J.B., Wallace, C.S.A. & Ravi, S. (2013) Phenology-based, remote sensing of post-burn disturbance windows in rangelands. *Ecological Indicators*, **30**, 35–44. https://doi.org/10.1016/j.ecolind.2013.02.004

Schindler, D.W. & Lee, P.G. (2010) Comprehensive conservation planning to protect biodiversity and ecosystem services in Canadian boreal regions under a warming climate and increasing exploitation. *Biological Conservation*, **143**, 1571–1586. https://doi.org/10.1016/j.biocon.2010.04.003

Serbin, S.P., Gower, S.T. & Ahl, D.E. (2009) Canopy dynamics and phenology of a boreal black spruce wildfire chronosequence. *Agricultural and Forest Meteorology*, **149**, 187–204. https://doi.org/10.1016/j.agrformet.2008.08.001

Serrouya, R., Dickie, M., DeMars, C., Wittmann, M.J. & Boutin, S. (2020) Predicting the effects of restoring linear features on woodland caribou populations. *Ecological Modelling*, **416**, 108891. https://doi.org/10.1016/j.ecolmodel.2019.108891

Seyednasrollah, B., Young, A.M., Hufkens, K., Milliman, T., Friedl, M.A., Frolking, S. et al. (2019) Tracking vegetation phenology across diverse biomes using Version 2.0 of the PhenoCam Dataset. *Scientific Data*, **6**, 222. https://doi.org/10.1038/s41597-019-0229-9

Sirén, A.P.K., Somos-Valenzuela, M., Callahan, C., Kilborn, J.R., Duclos, T., Tragert, C. et al. (2018) Looking beyond wildlife: using remote cameras to evaluate accuracy of gridded snow data. *Remote Sensing in Ecology and Conservation*, **4**, 375–386. https://doi.org/10.1002/rse2.85

Steenweg, R., Hebblewhite, M., Kays, R., Ahumada, J., Fisher, J.T., Burton, C. et al. (2017) Scaling-up camera traps: monitoring the planet's biodiversity with networks of remote sensors. *Frontiers in Ecology and the Environment*, **15**, 26–34. https://doi.org/10.1002/fee.1448

Steinaker, D.F., Jobbágy, E.G., Martini, J.P., Arroyo, D.N., Pacheco, J.L. & Marchesini, V.A. (2016) Vegetation composition and structure changes following roller-chopping deforestation in central Argentina woodlands. *Journal of Arid Environments*, **133**, 19–24. https://doi.org/10.1016/j.jaridenv.2016.05.005

Stewart, F.E.C., Fisher, J.T., Burton, A.C. & Volpe, J.P. (2018) Species occurrence data reflect the magnitude of animal movements better than the proximity of animal space use. *Ecosphere*, **9**, e02112. https://doi.org/10.1002/ecs2.2112

Tabak, M.A., Norouzzadeh, M.S., Wolfson, D.W., Sweeney, S.J., Vercauteren, K.C., Snow, N.P. et al. (2019) Machine learning to classify animal species in camera trap images: applications in ecology. *Methods in Ecology and Evolution*, **10**, 585–590. https://doi.org/10.1111/2041-210X.13120

Taddeo, S. & Dronova, I. (2018) Indicators of vegetation development in restored wetlands. *Ecological Indicators*, **94**, 454–467. https://doi.org/10.1016/j.ecolind.2018.07.010

Tattersall, E.R., Burgar, J.M., Fisher, J.T. & Burton, A.C. (2020a) Mammal seismic line use varies with restoration: applying habitat restoration to species at risk conservation in a working landscape. *Biological Conservation*, **241**, 108295. https://doi.org/10.1016/j.biocon.2019.108295

Tattersall, E.R., Burgar, J.M., Fisher, J.T. & Burton, A.C. (2020b) Boreal predator co-occurrences reveal shared use of seismic lines in a working landscape. *Ecology and Evolution*, **10**, 1678–1691. https://doi.org/10.1002/ece3.6028

Toomey, M., Friedl, M.A., Frolking, S., Hufkens, K., Klosterman, S., Sonnentag, O. et al. (2015) Greenness indices from digital cameras predict the timing and seasonal dynamics of canopy-scale photosynthesis. *Ecological Applications*, **25**, 99–115. https://doi.org/10.1890/14-0005.1

Torre Cerro, R. & Holloway, P. (2020) A review of the methods for studying biotic interactions in phenological analyses. *Methods in Ecology and Evolution*, **12**(2), 227–244. https://doi.org/10.1111/2041-210X.13519

Tóth, V.R. (2018) Monitoring spatial variability and temporal dynamics of phragmites using unmanned aerial vehicles. *Frontiers in Plant Science*, **9**, 1–11. https://doi.org/10.3389/fpls.2018.00728

Tuanmu, M.-N., Viña, A., Bearer, S., Xu, W., Ouyang, Z., Zhang, H. et al. (2010) Mapping understory vegetation using phenological characteristics derived from remotely sensed data. *Remote Sensing of Environment*, **114**, 1833–1844. https://doi.org/10.1016/j.rse.2010.03.008

Tuck, S.L., Phillips, H.R.P., Hintzen, R.E., Scharlemann, J.P.W., Purvis, A. & Hudson, L.N. (2014) MODISTools - downloading and processing MODIS remotely sensed data in R. *Ecology & Evolution*, **4**(24), 4658–4668.

van Rensen, C.K., Nielsen, S.E., White, B., Vinge, T. & Lieffers, V.J. (2015) Natural regeneration of forest vegetation on legacy seismic lines in boreal habitats in Alberta's oil sands region. *Biological Conservation*, **184**, 127–135. https://doi.org/10.1016/j.biocon.2015.01.020

Vartanian, M., Nijland, W., Coops, N.C., Bater, C., Wulder, M.A. & Stenhouse, G. (2014) Assessing the impact of field of view on monitoring understory and overstory phenology using digital repeat photography. *Canadian Journal of Remote Sensing*, **40**, 85–91. https://doi.org/10.1080/07038992.2014.930308

Visser, M.E. & Both, C. (2005) Shifts in phenology due to global climate change: the need for a yardstick. *Proceedings of the Royal Society B: Biological Sciences*, **272**, 2561–2569. https://doi.org/10.1098/rspb.2005.3356

Wagner, K.I., Gallagher, S.K., Hayes, M., Lawrence, B.A. & Zedler, J.B. (2008) Wetland restoration in the new millennium: do research efforts match opportunities? *Restoration Ecology*, **16**, 367–372. https://doi.org/10.1111/j.1526-100X.2008.00433.x

Wäldchen, J. & Mäder, P. (2018) Machine learning for image based species identification. *Methods in Ecology and Evolution*, **9**, 2216–2225. https://doi.org/10.1111/2041-210X.13075

Walker, J.J. & Soulard, C.E. (2019) Phenology patterns indicate recovery trajectories of ponderosa pine forests after high-severity fires. *Remote Sensing*, **11**, 2782. https://doi.org/10.3390/rs11232782

Webb, S.L., Gee, K.L., Strickland, B.K., Demarais, S. & DeYoung, R.W. (2010) Measuring fine-scale white-tailed deer movements and environmental influences using GPS Collar. *International Journal of Ecology*, 1–12. https://doi.org/10.1155/2010/459610

Westergaard-Nielsen, A., Lund, M., Pedersen, S.H., Schmidt, N.M., Klosterman, S., Abermann, J. et al. (2017) Transitions in high-Arctic vegetation growth patterns and ecosystem productivity tracked with automated cameras from 2000 to 2013. *Ambio*, **46**, 39–52. https://doi.org/10.1007/s13280-016-0864-8

Whittingham, M.J., Stephens, P.A., Bradbury, R.B. & Freckleton, R.P. (2006) Why do we still use stepwise modelling in ecology and behaviour? *Journal of Animal Ecology*, **75**, 1182–1189. https://doi.org/10.1111/j.1365-2656.2006.01141.x

Wittische, J., Heckbert, S., James, P.M.A., Burton, A.C. & Fisher, J.T. (2021) Community-level modelling of boreal forest mammal distribution in an oil sands landscape. *Science of The Total Environment*, **755**, 142500. https://doi.org/10.1016/j.scitotenv.2020.142500

Xu, R. (2003) Measuring explained variation in linear mixed effects models. *Statistics in Medicine*, **22**, 3527–3541. https://doi.org/10.1002/sim.1572

Yun, J., Jeong, S.-J., Ho, C.-H., Park, C.-E., Park, H. & Kim, J. (2018) Influence of winter precipitation on spring phenology in boreal forests. *Global Change Biology*, **24**, 5176–5187. https://doi.org/10.1111/gcb.14414

Zeng, L., Wardlow, B.D., Xiang, D., Hu, S. & Li, D. (2020) A review of vegetation phenological metrics extraction using time-series, multispectral satellite data. *Remote Sensing of Environment*, **237**, 111511. https://doi.org/10.1016/j.rse.2019.111511

Zhang, X., Friedl, M.A., Schaaf, C.B., Strahler, A.H., Hodges, J.C.F., Gao, F. et al. (2003) Monitoring vegetation phenology using MODIS. *Remote Sensing of Environment*, **84**, 471–475. https://doi.org/10.1016/S0034-4257(02)00135-9

Zhao, B., Donnelly, A. & Schwartz, M.D. (2020) Evaluating autumn phenology derived from field observations, satellite data, and carbon flux measurements in a northern mixed forest, USA. *International Journal of Biometeorology*, **64**, 713–727. https://doi.org/10.1007/s00484-020-01861-9

Zimova, M., Hackländer, K., Good, J.M., Melo-Ferreira, J., Alves, P.C. & Mills, L.S. (2018) Function and underlying mechanisms of seasonal colour moulting in mammals and birds: what keeps them changing in a warming world? *Biological Reviews*, **93**, 1478–1498. https://doi.org/10.1111/brv.12405

Zimova, M., Mills, L.S. & Nowak, J.J. (2016) High fitness costs of climate change-induced camouflage mismatch. *Ecology Letters*, **19**, 299–307. https://doi.org/10.1111/ele.12568

Supporting Information

Additional supporting information may be found online in the Supporting Information section at the end of the article.

Table S1. Description of the linear models used to assess vegetation dynamics (phenology and productivity) across sampling strata (Control, Human Use, Active restoration, Passive restoration, Offline) or wildlife habitat use, with data collected at n = 73 camera trap (CT) sites and satellites in the study area in northern Alberta, Canada, from January 2016 to November 2019.

Table S2. Model set for identifying the most supported variance and dispersion structure under a negative binomial response distribution for weekly crane, caribou, and deer counts per site at n = 73 camera trap (CT) sites in the study area in northern Alberta, Canada, from January 2016 to November 2019.

Table S3. Model selection results for weekly crane, caribou, and deer counts per site at n = 73 camera trap (CT) sites in the study area in northern Alberta, Canada, from January 2016 to November 2019.

Table S4. Model set for identifying the most supported variance and dispersion structure under a negative binomial response distribution for 16-day crane, caribou, and deer counts per site at n = 73 CT sites in the study area

in northern Alberta, Canada, from January 2016 to November 2019.

Table S5. Full model selection results for 16-day crane, caribou, and deer counts per site at n = 73 CT sites in the study area in northern Alberta, Canada, from January 2016 to November 2019.

Table S6. Model set for identifying the most supported variance and dispersion structure under a negative binomial response distribution for annual sandhill crane, woodland caribou, and white-tailed deer counts per site at n = 73 camera trap (CT) sites in the study area in northern Alberta, Canada, from January 2016 to November 2019.

Table S7. Model selection results for camera-based phenology covariates on annual crane, caribou, and deer counts per site at n = 73 camera trap (CT) sites in the study area in northern Alberta, Canada, from January 2016 to November 2019.

Table S8. Model selection results for NDVI (satellite, MODIS 250 m) productivity covariates on annual crane, caribou, and deer counts per site at n = 73 camera trap (CT) sites in the study area in northern Alberta, Canada, from January 2016 to November 2019.

Table S9. Model selection results for EVI (satellite, MODIS 250 m) productivity covariates on annual crane, caribou, and deer counts per site at n = 73 camera trap (CT) sites in the study area in northern Alberta, Canada, from January 2016 to November 2019.

Table S10. Habitat model selection results for annual crane, caribou, and deer counts per site at n = 73 camera trap (CT) sites in the study area in northern Alberta, Canada, from January 2016 to November 2019.

Table S11. Anthropogenic model selection results for annual crane, caribou, and deer counts per site at n = 73 camera trap (CT) sites in the study area in northern Alberta, Canada, from January 2016 to November 2019.

Table S12. Number of independent detection events per species in each sampling stratum and habitat type, across n = 73 camera trap (CT) sites in the study area in northern Alberta, Canada, from January 2016 to November 2019.

Figure S1. Example images showing the automated process for extracting understory vegetation phenology and productivity patterns from camera trap (CT) time-lapse images at a site.

Figure S2. Spline curves fit to the greenness indices extracted from understory vegetation across 5 sampling strata at n = 73 camera trap (CT) sites in the study area in northern Alberta, Canada, from January 2016 to November 2019.

Figure S3. Images of the 3 species, including (A) white-tailed deer, (B) sandhill crane, and (C) caribou, at camera trap sites during summer periods, i.e., the peak periods of vegetation growth, in the study area in northern Alberta, Canada, from January 2016 – November 2019.

Figure S4. Plots to determine for each species the threshold minimum number of detections per camera trap (CT) site used to measure concordance between repeated wildlife habitat use and understory vegetation phenology.

Figure S5. Number of total independent detections per week of sandhill crane, woodland caribou, and white-tailed deer at n = 73 camera trap (CT) sites across sampling strata in the study area in northern Alberta, Canada from January 2016 to November 2019.

Figure S6. Number of total independent detections per month per camera trap (CT) site of sandhill crane, woodland caribou, and white-tailed deer across n = 73 CT sites for each of the sampling strata in the study area in northern Alberta, Canada from January 2016 to November 2019.

Figure S7. Histogram of Pearson correlations between greenness measured by CTs at n=73 CT sites and EVI and NDVI.

Supplementary Text

